

# Effect of Mono- and Multivalent Salts on Angle-dependent Attractions between Charged Rods

Kun-Chun Lee<sup>1</sup>, Itamar Borukhov<sup>1</sup>, William M. Gelbart<sup>1</sup>, Andrea J. Liu<sup>1</sup>, and Mark J. Stevens<sup>2</sup>

<sup>1</sup>*Dept. of Chemistry and Biochemistry, University of California, Los Angeles, CA 90095-1569*

<sup>2</sup>*Sandia National Laboratories, Albuquerque, NM 87185-1411*

Using molecular dynamics simulations we examine the effective interactions between two like-charged rods as a function of angle and separation. In particular, we determine how the competing electrostatic repulsions and multivalent-ion-induced attractions depend upon concentrations of simple and multivalent salt. We find that with increasing multivalent salt the stable configuration of two rods evolves from isolated rods to aggregated perpendicular rods to aggregated parallel rods; at sufficiently high concentration, additional multivalent salt reduces the attraction. Monovalent salt enhances the attraction near the onset of aggregation, and reduces it at higher concentration of multivalent salt.

PACS numbers: 87.15.-v, 82.35.Rs, 81.16.Dn, 87.16.Ka

Multivalent-ion-induced aggregation of stiff polyelectrolytes has been studied extensively in recent years for at least two important reasons: it arises from correlations not included at the mean-field (Poisson-Boltzmann) level [1, 2, 3, 4, 5, 6, 7, 8, 9], and it lies at the heart of biological phenomena such as cytoskeleton re-organization [10, 11, 12] and DNA packaging [13, 14]. Most studies have focused exclusively on the interaction between charged rods that are parallel. A few theoretical calculations have allowed for non-parallel orientations [15, 16], but only at a single multivalent salt concentration. Recent work [17, 18, 19], however, suggests that the *evolution* of angle-dependent attractions with changing multivalent salt concentration is crucial to phase behavior. For example, at intermediate multivalent salt concentrations F-actin solutions can form lamellar phases of stacked rafts where each raft consists of two layers of mutually perpendicular actin filaments, but at higher multivalent salt concentrations they form bundles of nearly parallel filaments [19]. Similar physics may apply to transitions from networks to bundles of F-actin in the cytoskeleton [18].

In this study we use explicit-ion, continuum-dielectric molecular dynamics (MD) simulations to examine how the concentrations of monovalent and multivalent salts affect the angle- and distance-dependent effective potential between two charged rods. A threshold concentration of multivalent salt is needed for the two rods to attract. We find that the preferred configuration is perpendicular just above the threshold, and parallel at higher concentrations of multivalent salt, in agreement with the experiments on F-actin solutions cited above [19]. Furthermore, monovalent salt can lower the concentration of multivalent salt needed for attraction, suggesting that monovalent salt may induce aggregation. Finally, we find that the rods can still attract even when they are overcharged [9] (i.e. the sign of their effective charge is reversed by condensed counterions) at high multivalent salt concentrations, and that the attraction weakens

with increasing overcharging. However, we never observe strong overcharging because above a certain concentration of multivalent salt the added multivalent ions simply form complexes with monovalent co-ions in solution [20].

In our simulations each rod is composed of 64 spherical monomers, each carrying a charge of  $-1$  in units of the electronic charge  $e$ , separated at fixed intervals. The two rods are perfectly rigid and fixed at a specified center-to-center separation,  $R$ , and angle  $\gamma$ . In all cases, one rod lies parallel to the face diagonal of the enclosing periodic box [21], while the other is rotated away from a parallel configuration at an angle  $\gamma$  about the axis connecting the centers of the rods. In addition, we introduce mobile multivalent ions of charge  $+3$ , and mobile monovalent ions of charges  $+1$  and  $-1$ . The system is always electrostatically neutral, with 128 ions of charge  $+1$  to balance the charge on the two rods, one ion of charge  $-1$  for every additional ion of charge  $+1$  (monovalent or 1:1 salt), and 3 ions of charge  $-1$  for every ion of charge  $+3$  (trivalent or 3:1 salt).

We reference salt concentrations to the total charge on the two rods (128 electronic charges). For example, a 3:1 salt concentration of  $c_{3:1} = 1$  means that the total charge due to  $+3$  ions is equal to the total charge on the two rods. Similarly, a 1:1 salt concentration of  $c_{1:1} = 1$  means that the total charge due to  $+1$  ions from the monovalent salt is equal to the total charge of the two rods.

We include two types of pair interactions between particles. First, we use the truncated Lennard-Jones potential to allow for short-range repulsions. This introduces the energy scale  $\epsilon$  and the particle size  $\sigma$ . Second, we include the Coulomb interaction,  $Z_1 Z_2 / \epsilon r_{12}$ , where  $Z_i$  is the charge on particle  $i$  and  $\epsilon$  is the dielectric constant. To handle the long-range Coulomb interaction in our system with periodic boundaries we use the Particle Mesh Ewald (PME) method [22].

Our simulations are carried out in the canonical (NVT) ensemble with the temperature fixed at  $k_B T = 1.2\epsilon$  us

ing the Langevin thermostat [23]. The monomer number density,  $10^{-4}\sigma^{-3}$ , corresponds to a box volume of  $(109\sigma)^3$ . The dielectric constant is chosen such that the Bjerrum length (the distance at which the electrostatic interaction between two electronic charges is equal to the thermal energy) is  $l_B \equiv 1/\epsilon k_B T = 3.2\sigma$ . The separation between charges on the rod (i.e., the monomer separation) is  $l = 1.1\sigma$  and the dimensionless Oosawa-Manning ratio [1, 24] is  $l_B/l = 2.9$ , well above the threshold for counterion condensation.

The characteristic time scale for the simulation is  $\tau = \sqrt{m\sigma^2/\epsilon}$ , where  $m$  is the particle mass. We use the leapfrog-Verlet integration scheme with a time step of  $0.01\tau$ . Each simulation run is equilibrated (as measured by the leveling-off of the energy) for at least  $10^3\tau$  before we collect data. The force on each monomer is then averaged over  $40\tau$  intervals until we obtain 250–450 average-force data points. More extended runs were performed for a few systems to check that our results are not affected by the choice of equilibration time, time step or data collection interval. For each simulation run we calculate both the average normal force per monomer between the two rods and the average torque on the rods about the center-to-center axis. Error bars (indicated by the size of the points in our figures) correspond to the statistical error associated with the average forces at each  $40\tau$  interval.

To obtain the effective interaction potential, or reversible work, as a function of the separation  $R$  between the two rods, we should integrate the normal force with distance as the rods are brought from infinite separation to  $R$  at fixed angle  $\gamma$ . This is not possible within our periodic-boundary-condition simulation. Instead, we calculate the reversible work,  $\Delta W(R)$ , for bringing the two rods from a fixed reference separation [25] of  $8\sigma$  to  $R$  at fixed  $\gamma$ . Similarly, the effective potential as a function of angle,  $\Delta W(\gamma)$ , is calculated by integrating the torque from  $90^\circ$  to  $\gamma$  at fixed  $R$ .

We first ask how the effective interaction between two charged rods depends on the concentration of multivalent salt, in the absence of monovalent salt. Fig. 1(a) shows a plot of the effective potential per monomer,  $\Delta W$ , as a function of separation,  $R$ , when the two rods are parallel ( $\gamma = 0^\circ$ ). In the absence of 3:1 salt  $\Delta W(R)$  is positive for all  $R$ , implying that the rods repel. When enough 3:1 salt is added ( $c_{3:1} \approx 0.3$ ), the effective potential develops a global minimum at small  $R$ ; the rods now attract each other. This is the threshold 3:1 salt concentration for aggregation; note that this corresponds to approximately only one-third of the charge on the rods neutralized by trivalent ions. Beyond this threshold the attraction increases with multivalent salt concentration until  $c_{3:1} = 1$ ; this is where the charge on the rods is completely neutralized by the trivalent counterions. Beyond  $c_{3:1} = 1$ , the attraction decreases slightly (short-dashed curve;  $c_{3:1} = 12$ ). Thus, the magnitude of the

attraction is non-monotonic with 3:1 salt [26]. Similar non-monotonicity is observed in experiments with mixed salts on DNA solutions [27]. Though it is imperceptible in the figure, the effective potential beyond  $4.5\sigma$  is positive for both  $c_{3:1} = 1$  and  $c_{3:1} = 12$ , which means that the rods still repel one another at large distance.

The angle dependence of the effective rod-rod interaction is shown in Fig. 1(b) for  $R = 2.1\sigma$ , near the attractive minimum. In the absence of 3:1 salt the rods prefer to be perpendicular since the rods repel one another. Just above the threshold for aggregation (solid curve), the global minimum is at  $90^\circ$ , implying that the preferred aggregated configuration is a cross. As the concentration of multivalent salt increases further the minimum at  $\gamma = 0^\circ$  deepens, and at  $c_{3:1} = 1$  the rods now prefer to aggregate in a parallel configuration. When still more multivalent salt is added the minimum at small angle decreases; this shows again that the effective potential depends non-monotonically on the concentration of multivalent salt.

In many-rod systems under conditions for which a pair of rods prefers to aggregate perpendicularly, we would expect to find networks, rafts or other structures where rods cross each other at large angles. On the other hand, when a pair prefers to aggregate in a parallel configuration, we expect to find bundles or networks of bundles. Note that for a pair of rods, the preferred angle at which they aggregate does not vary continuously with increasing multivalent salt as it would at zero temperature, but rather jumps from  $90^\circ$  to  $0^\circ$ . This entropic effect suggests that transitions from network/raft structures to bundles may be first-order [18].

Fig. 2 shows the effects of added monovalent salt on the effective interaction at a multivalent salt concentration of  $c_{3:1} = 0.3$ , just above the threshold for aggregation. In Fig. 2(a) the attraction is seen to grow stronger with increasing 1:1 salt. Furthermore, we find (not shown) that if the 3:1 salt concentration is *below* threshold, then 1:1 salt can actually drive the pair to aggregate. Fig. 2(b) shows that the metastable minimum at  $0^\circ$  increases in depth and becomes the global minimum with increasing 1:1 salt. This result suggests that adding 1:1 salt to a solution of charged rods in a network or raft phase can drive the solution into the bundle phase. To our knowledge, an experiment has not yet been designed to test these two effects of added 1:1 salt.

To see why monovalent salt enhances the effective attraction, we measure the neutralization fraction,  $f(r_c)$ , defined as the time average of the sum of all mobile charges, positive and negative, within radius  $r_c$  from either one of the rods, divided by the total charge of a rod [28]. The sketches in Fig. 3 depict a top view of the volume that encompasses the mobile charges included in the calculation of  $f(r_c)$  for a given  $r_c$  and separation  $R$ . For  $r_c < R/2$  (to the left of the vertical dotted line), there are two separate enclosing volumes, as sketched, while for

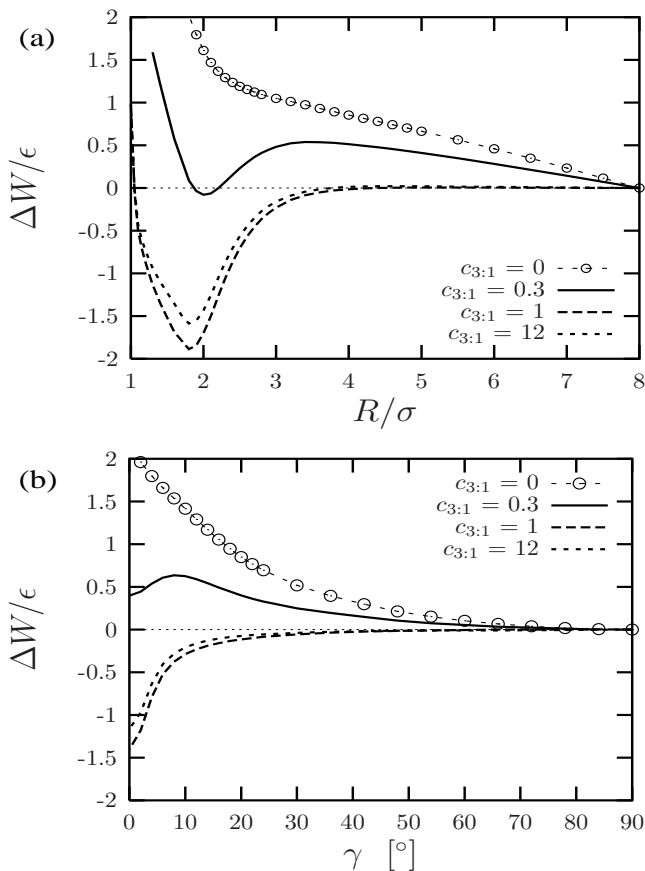


FIG. 1: (a) The effective potential,  $\Delta W(R)$ , between two parallel charged rods for different concentrations of multivalent salt. The size of the solid circles at  $c_{3:1} = 0$  corresponds to the error bar for all points on all curves. (b) The effective potential,  $\Delta W$ , as a function of angle,  $\gamma$ , for two rods separated by  $R = 2.1\sigma$ , for different concentrations of multivalent salt.

$r_c > R/2$  (right of the vertical line), the two enclosing volumes merge into one. Fig. 3 shows  $f(r_c)$  for different concentrations of 1:1 and 3:1 salts. The solid (dashed) curves correspond to cases without (with) 1:1 salt. Near the 3:1 salt threshold for aggregation,  $c_{3:1} = 0.3$ , the solid and dashed black curves show that  $f(r_c)$  increases with added 1:1 salt. We find that the effective charge on the rods is reduced by nearby counterions from the 1:1 salt while the concentration of multivalent counterions near the rods is nearly unchanged [20]. As a result, the repulsive contribution to the effective interaction between rods is reduced while the attractive contribution is unaffected, giving rise to the increase in the net effective attraction shown in Fig. 2. (Note that for the black dashed curve, the screening length—about  $6\sigma$ —is significantly larger than the inter-rod separation of  $R = 3.6\sigma$  and hence not relevant here.)

At high concentrations of multivalent salt ( $c_{3:1} \geq 1$ ), we find that monovalent salt has the opposite effect—it ac-

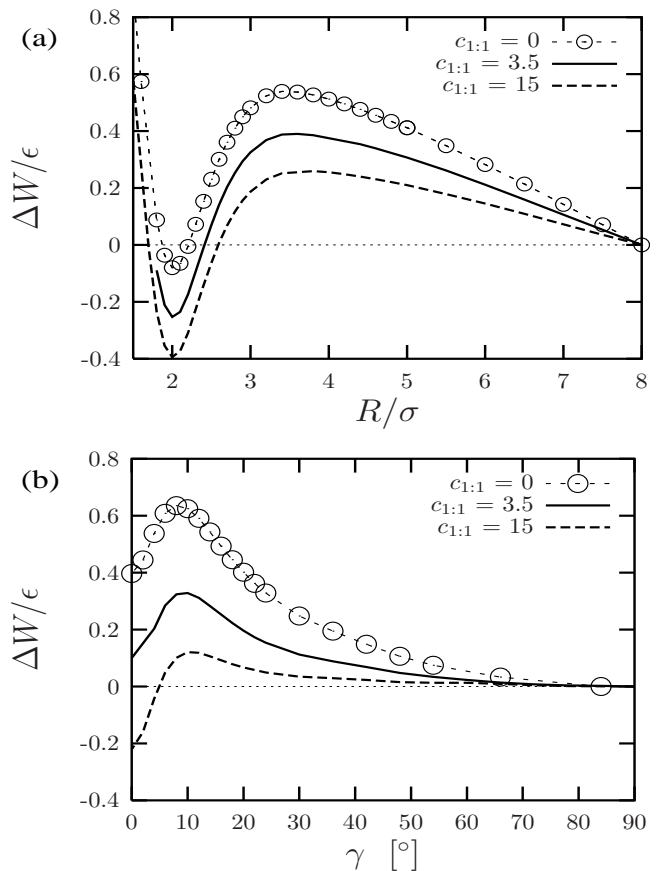


FIG. 2: The effective potential between two charged rods,  $\Delta W$  as a function of (a) separation  $R$  for parallel rods ( $\gamma = 0^\circ$ ) and (b) angle  $\gamma$  for closely-separated rods ( $R = 2.1\sigma$ ), for different monovalent salt concentrations. The multivalent salt concentration is fixed at  $c_{3:1} = 0.3$ , just above the threshold for aggregation. The size of the solid circles at  $c_{1:1} = 0$  indicates the error bar for all points on all curves.

tually *reduces* the effective attraction. This is consistent with experiments on DNA solutions [27]. This effect also can be understood by looking at  $f(r_c)$ . The gray solid and dashed curves in Fig. 3 show that  $f(r_c)$  decreases with added 1:1 salt, consistent with earlier predictions [20]. Furthermore, we find that fewer multivalent ions contribute to  $f(r_c)$  upon the addition of 1:1 salt because the multivalent ions stay in solution in the form of complexes with monovalent co-ions. We conclude that co-ions lure multivalent ions away from the two rods, causing the attraction to decrease.

The top curve (dotted) in Fig. 3 shows that overcharging occurs ( $f(r_c) > 1$ ) at sufficiently high concentrations of multivalent salt. Note that  $f(r_c)$  crosses 1 at  $r_c \approx 1.3\sigma$ . Since  $R > 2r_c$  at this point (the situation sketched to the left of the vertical dotted line), the total charge enclosed in each cylinder shown is now positive and the rods are overcharged [9]. This overcharging saturates with 3:1 salt; we find, for example, that when the multivalent salt

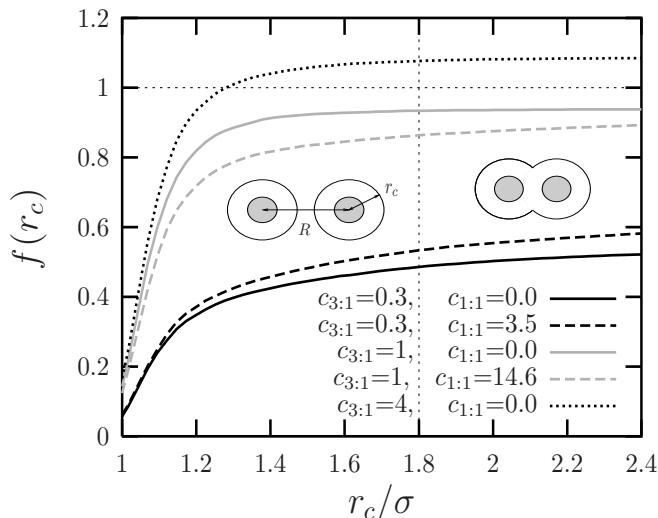


FIG. 3: Neutralization fraction  $f$  for 2 parallel rods at  $R = 3.6\sigma$  as a function of the radius of the encompassing volume  $r_c$  for several different concentrations of multivalent and monovalent salts. The vertical dotted line corresponds to  $r_c = R/2$ ; to its left, we sum the mobile charges enclosed in two separate volumes, as sketched in top view, while to the right, we sum the mobile charges enclosed in a single volume with a figure-eight cross-section.

concentration is tripled from  $c_{3:1} = 4$  to  $c_{3:1} = 12$  there is only a few percent increase in  $f(r_c)$ . Beyond a certain concentration of 3:1 salt, additional multivalent ions stay in solution in the form of complexes with oppositely-charged monovalent ions. As a result, we never observe strong overcharging.

Fig. 1 shows that overcharging weakens the effective attraction. At first glance this is not surprising because overcharging should increase the Coulomb repulsion [9]. However, when we increase the 3:1 salt concentration above  $c_{3:1} = 1.0$  we find that the normal force between rods (which we integrate to obtain the effective interaction) remains negligibly small at large separations, whereas it becomes significantly less negative at small separations. This implies that overcharging does not affect the contribution of the longer-ranged Coulomb repulsion but appreciably weakens the contribution of counterion-mediated attractions to the effective interaction. Fig. 3 suggests why the repulsion is not significantly affected by overcharging:  $f(r_c)$  is approximately as far above unity for  $c_{3:1} = 4$  as it is below unity for  $c_{3:1} = 1$ . Thus, the magnitude of the total charge enclosed within  $r_c$  is the same in the two cases although the sign of the charge has flipped.

How then does overcharging weaken the counterion-mediated attraction? As the concentration of multivalent salt increases, the amount of condensed charge increases slightly by accumulating primarily on the far sides of the rods. We find that this reorganization of charge (from

"bonding" to "antibonding" regions) leads to a decrease of the attraction.

We thank Markus Deserno and David Reguera for instructive discussions. This work was supported by NSF-CHE-0096492 (AJL), NSF-CHE-9988651 (WGM), and DE-AC04-94AL85000 (MJS).

- 
- [1] F. Oosawa, *Biopolymers* **6**, 1633 (1968).
  - [2] L. Guldbraend, L. G. Nilsson, and L. Nordenskiöld, *J. Chem. Phys.* **85**, 6686 (1986).
  - [3] I. Rouzina and V. A. Bloomfield, *J. Phys. Chem.* **100**, 9977 (1996).
  - [4] N. Grønbech-Jensen, R. J. Mashl, R. F. Bruinsma, and W. M. Gelbart, *Phys. Rev. Lett.* **78**, 2477 (1997).
  - [5] B.-Y. Ha and A. J. Liu, *Phys. Rev. Lett.* **79**, 1289 (1997).
  - [6] J. J. Arenzon, J. F. Stilck, and Y. Levin, *Eur. Phys. J. B* **12**, 79 (1999).
  - [7] F. J. Solis and M. Olvera de la Cruz, *Phys. Rev. E* **60**, 4496 (1999).
  - [8] M. J. Stevens, *Phys. Rev. Lett.* **82**, 101 (1999).
  - [9] T. T. Nguyen, I. Rouzina, and B. I. Shklovskii, *J. Chem. Phys.* **112**, 2562 (2000).
  - [10] T. D. Pollard, *Ann. Rev. Biochem.* **55**, 987 (1986).
  - [11] P. A. Janmey, S. Hvidt, J. Lamb, and T. P. Stossel, *Nature* **345**, 89 (1990).
  - [12] E. Sackmann, *Semin. Cell Dev. Biol.* **7**, 707 (1996).
  - [13] J. Widom and R. L. Baldwin, *Biopolymers* **22**, 1595 (1983).
  - [14] V. A. Bloomfield, *Biopolymers* **31**, 1471 (1991).
  - [15] B.-Y. Ha and A. J. Liu, *Eur. Phys. Lett.* **46**, 624 (1999).
  - [16] J. F. Stilck, Y. Levin, and J. J. Arenzon, *J. Stat. Phys.* **106**, 287 (2002).
  - [17] I. Borukhov and R. F. Bruinsma, *Phys. Rev. Lett.* **87**, 158101 (2001).
  - [18] I. Borukhov, R. F. Bruinsma, W. M. Gelbart, and A. J. Liu, preprint.
  - [19] G. C. L. Wong, A. Lin, J. X. Tang, Y. Li, P. A. Janmey, and C. R. Safinya, *Phys. Rev. Lett.* **91**, 018103 (2003).
  - [20] P. González-Mozuelos and M. Olvera de la Cruz, *J. Chem. Phys.* **118**, 4684 (2003).
  - [21] Because of periodic boundary conditions our results depend slightly on the absolute orientation of the two rods, but none of our qualitative conclusions are affected by a particular choice of orientation.
  - [22] H. G. Petersen, *J. Chem. Phys.* **103**, 3668 (1995).
  - [23] J. M. Thijssen, *Computer Physics* (Cambridge University Press, 1999).
  - [24] G. S. Manning, *Quarterly Reviews of Biophysics* **11**, 179 (1978).
  - [25] At the threshold, 3:1 = 0.3, the reversible work for bringing the two rods from the box boundary to a separation of  $8\sigma$  is at most about  $0.5\epsilon < k_B T$ .
  - [26] J. Z. Wu, D. Bratko, H. W. Blanch, and J. M. Prausnitz, *J. Chem. Phys.* **111**, 7084 (1999).
  - [27] E. Raspaud and F. Livolant (2003), preprint. This experiment measures the center-to-center spacing,  $d$ , of DNA condensed into bundles. If one makes the reasonable assumption that  $d$  increases when the counterion-mediated attraction weakens relative to the electrostatic repulsion then our results are fully consistent with theirs.

[28] We have checked that the  $f(r_c)$  of each rod is the same.